

A RESILIENT CLT SHEAR WALL SYSTEM FOR TIMBER BUILDINGS

Chenhui Qian¹, Fei Tong², Thomas Tannert³, Leo Panian⁴, Mike Korolyk⁵, Anurag Upadhyay⁶

ABSTRACT: Balloon-framed cross-laminated timber (CLT) walls are gaining traction as seismic-force-resisting systems due to their capacity for self-centering and low-damage performance. This study proposes a novel balloon-framed rocking CLT shear wall system that employs non-proprietary hysteretic metallic dampers to enhance energy dissipation and resilience under seismic loading. The proposed system allows rocking at the base of central wall panels while energy is dissipated through yielding fuse plates (YFPs) located along spline joints. A mechanics-based analytical model is developed to describe the lateral stiffness and base shear capacity of the system. The model is validated using nonlinear pushover analysis in OpenSees, which incorporates rigid diaphragm assumptions and custom damper behavior. Numerical results show that the proposed system can deliver stable, predictable mechanical response with accurate predictions of base shear capacity, and that the dampers' yield strengths should be equally distributed along the height for mid-wise buildings. The findings contribute to the development of resilient timber structures and offer a viable path toward seismic design modernization for mass timber buildings.

KEYWORDS: Cross-laminated timber ; Rocking shear wall; Hysteretic dampers; Balloon-framed system

1 – INTRODUCTION

1.1 CLT SEISMIC-FORCE-RESISTING SYSTEM

Cross-laminated timber (CLT) is increasingly utilized in the construction of seismic-force-resisting system (SFRRS), offering two configurations: platform-type and balloon-type. Current North American wood design standards [1-3] aim to ensure global ductile behavior in platform-type assemblies with CLT panels remaining elastic while metallic connections providing ductility and energy dissipation. The seismic force reduction factor, R is specified as 4.0 in ASCE 7 [4] and as 2.0 in NBCC [5] for platform-type CLT shear wall systems. These provisions limit the efficiency of this SFRRS, leading to inefficient designs and rendering applications uneconomical and impractical. Furthermore, the prescribed failure mechanisms by these standards may result in unreliable energy dissipation and ductility due to brittle failures in fasteners and anchor connections.

To address these limitations, researchers have proposed balloon-framed rocking CLT shear wall systems to achieve seismic resilience. These systems are designed to rock at the base during earthquakes when the base overturning moment exceeds a predetermined threshold, thereby eliminating story

mechanisms and reducing inelastic drifts to better protect the structure. Such systems can also re-center post-earthquake, relying on restoring forces from gravity loads or vertical pre-stressing, thus eliminating permanent deformations and enhancing resilience. Two types of rocking CLT shear wall systems as alternatives to prescriptive code-based systems, have been developed: post-tensioned (PT) CLT walls [6-11] and systems incorporating self-centering dampers [12-14].

PT systems, illustrated in Figure 1, consist of CLT panels with PT tendons anchored at both the top and foundation levels. Energy dissipation devices, such as U-shaped flexural plates (UFPs), are commonly integrated to provide additional energy dissipation. However, PT systems may require significant repairs after major seismic events due to potential damage to energy dissipation devices, loss of pre-stress in PT tendons, and toe crushing of CLT panels [6-11]. To mitigate toe-crushing, curved-base rocking walls have been proposed as alternatives to conventional rectangular walls [15]. Additionally, the PT technique might be limited in mass timber structures due to the comparatively lower compressive resistance of wood versus concrete.

¹ Chenhui Qian, School of Engineering, University of Northern British Columbia, Prince George, Canada, bqian@unbc.ca

² Fei Tong, School of Engineering, University of Northern British Columbia, Prince George, Canada, fei.tong@unbc.ca

³ Thomas Tannert, School of Engineering, University of Northern British Columbia, Prince George, Canada, thomas.tannert@unbc.ca

⁴ Leo Panian, Tipping Structural Engineers, Berkeley, USA, l.panian@tippingstructural.com

⁵ Mike Korolyk, Tipping Structural Engineers, Berkeley, USA, m.korolyk@tippingstructural.com

⁶ Anurag Upadhyay, Tipping Structural Engineers, Berkeley, USA, a.upadhyay@tippingstructural.com

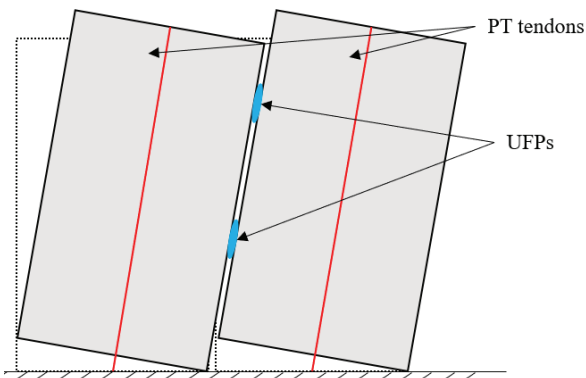


Figure 1. Typical post-tensioned CLT shear wall system

Parallel to PT system developments, Hashemi et al. [12-14] introduced balloon-type CLT shear wall systems with self-centering friction dampers in single-panel and coupled-panel configurations, respectively, as shown in Figure 2. These dampers provide built-in restoring forces and passive energy dissipation through friction, exhibiting a flag-shaped hysteresis. This hysteresis is characterized by high initial stiffness and distinct activation points when internal friction is overcome. While these systems exhibit considerably less damage than PT systems, the CLT panels remain at risk of damage when rocking about their toes.

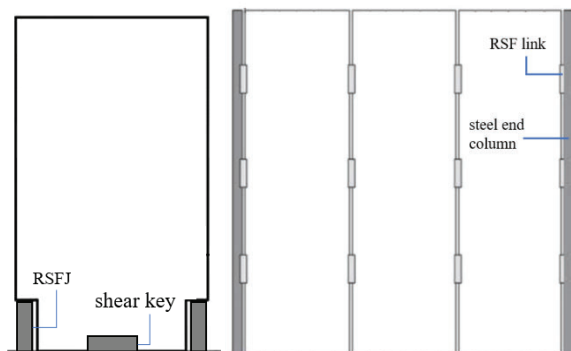


Figure 2. CLT shear wall with self-centering friction dampers: Single-panel (left) and coupled-panel (right)

1.2 OBJECTIVE

In this paper, an alternative rocking CLT shear wall system that employs hysteretic metallic dampers for energy dissipation is presented. The system aims to fully utilize the strength of CLT panels and to provide reliable ductility and energy dissipation. Furthermore, it seeks to achieve significant gains in efficiency and performance over conventional platform-framed CLT shear walls with steel plate connections, while alleviating potential issues associated with existing rocking CLT shear wall systems.

2 – BALLOON-FRAMED ROCKING CLT SHEAR WALL SYSTEM

2.1 CONCEPT AND CONFIGURATION

The proposed system comprises three CLT panels that are connected via ductile steel connectors along their joints, as shown in Figure 3. In this assembly, the central wall rests atop the foundation and is allowed to rock about its toes at the base. Both side panels are coupled with the central wall on their interior edge and designed to pivot about their exterior base corner where they are supported through a single pin. This pivoting action is not restricted at the interior base corner, where the side panels are detached from the foundation.

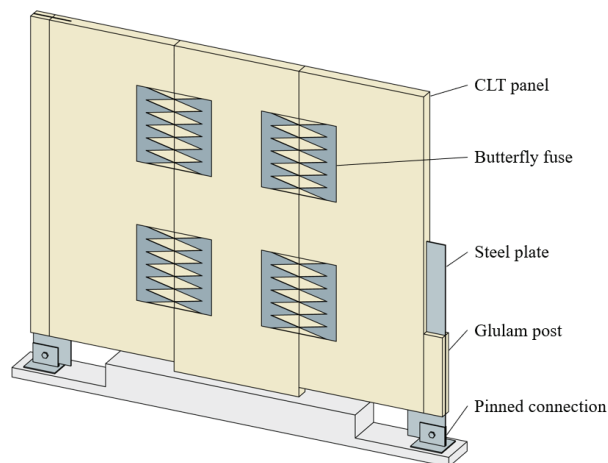


Figure 3. Schematic of the proposed rocking CLT shear wall system

Subjected to lateral loads, the CLT assembly drifts uniformly, leading to the central wall leaning towards its leeward rocking toe and the steel connectors being sheared along the joints. At this moment, the lateral resistance of the entire assembly relies on the rocking moment of the central wall and the push-and-pull action occurring at the two exterior pin supports. As the lateral load increases to a pre-designated level, the rocking action of the central wall is activated, with the ductile steel connectors yielding to act as shear fuses providing energy dissipation. As such, the nonlinear response of the CLT shear wall system is engaged, with the walls' tributary gravity loads providing re-centering capacity.

In the whole process, the side panels transfer forces between the shear fuses and the exterior pin supports. To prevent CLT failure at the pin supports, the embedded plates extend over a sufficient height to accommodate the self-tapping screws or glued-in rods required to resolve the reaction forces in the CLT panels. Both the pin connections and boundary elements are capacity protected to remain elastic.

There are multiple options to implement the shear fuses. One involves a series of YFPs with trapezoidal cutouts, forming a butterfly-shaped profile, as shown in Figure 3. Ma et al. [16] conducted a series of full-scale experiments on this butterfly fuse and quantified the impact of a few design parameters including the yield strength of the steel, the number of links, and the aspect ratio and the slenderness of the links. Another option is to use UFPs whose cyclic performance has been investigated as a function of their geometry [17].

2.2 BASIC MECHANICS

To understand the basic mechanics of the proposed system, an analytical model is developed for a two-story assembly, as illustrated in Figure 4a). This assembly is subjected to lateral loads applied at both floor and roof levels to simulate seismic inertial forces. The magnitudes of these forces follow an inverted triangular distribution over the height, maintaining a constant ratio of 1:0.5 between the roof and floor levels. While the direction of these forces is shown from left to right, conclusions of this paper are valid in the case where the loading is reversed.

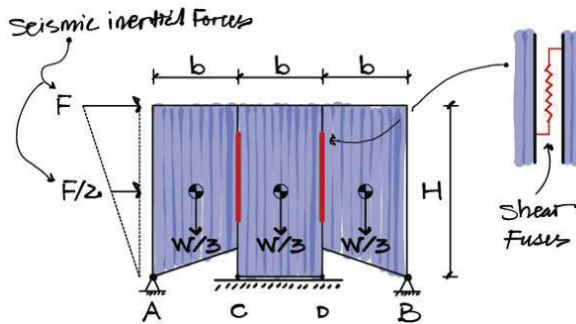


Figure 4. Analytical model of two-story system

In the vertical direction, the wall assembly supports a total tributary gravity load, W , including its self-weight as well as loads from the floor and roof levels. For simplicity, it is assumed that the total gravity load W is evenly distributed across the three panels, with each panel carrying $W/3$.

Given their high in-plane stiffness, all the CLT panels are assumed to behave as rigid bodies. Upon engagement, the side panels pivot about pins A and B, respectively, while the central wall rocking alternately about its toes at points C and D. These rigid-body rotations are made compatible through the floor and roof slabs as well as the shear fuses at the spline joints of the panels.

The floor and roof slabs are assumed to act as rigid diaphragms, leading to identical horizontal displacements at each level. Consequently, the applied lateral loads are entirely transferred and distributed to the wall panels in

proportion to their lateral stiffnesses, which reflects the distribution of seismic inertial forces in reality.

The shear fuses carry no horizontal forces across the wall panels but are only engaged to transfer shear forces along the spline joints. For mathematical convenience, they are lumped at each spline joint and modeled using a nonlinear spring. Each spring is assigned an elastic-perfectly plastic force-deformation relationship, characterized by a yield strength F_y and an initial stiffness K_0 , representing generic metallic dampers.

The lateral stiffnesses of the wall panels are the key to evaluating the demands on the pivotal pins, rocking toes, shear fuses, and screwed boundary elements, which can govern different limit states. To quantify these stiffnesses, free-body diaphragms are plotted for the left (LT), central (CT), and right (RT) wall panels, as shown in Figure 5.

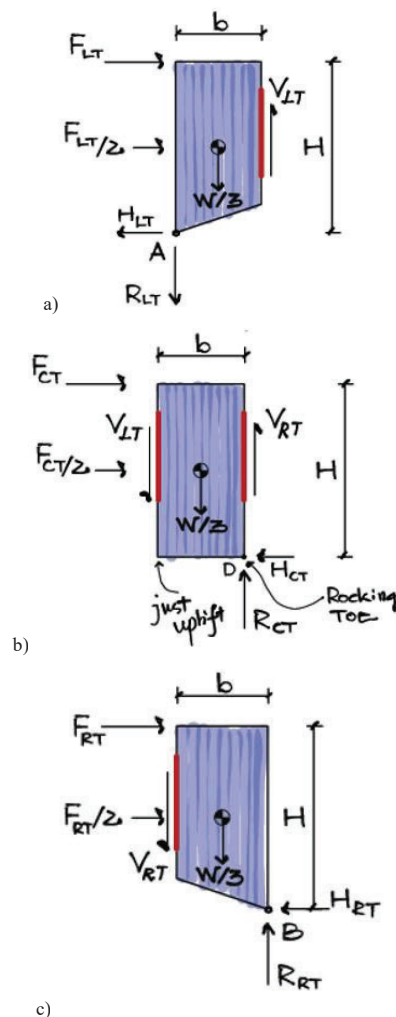


Figure 5. Free-body diaphragms of the CLT wall panels: a) left panel; b) central panel; c) right panel.

The intended yield/nonlinear mechanism of the proposed system involves the rocking of the central wall concurring with yielding in the shear fuses. Accordingly, the lateral stiffnesses of the three panels, k_{iT} , are evaluated at the onset of nonlinearity – when rocking is just activated and the first yielding is about to occur in the shear fuses, as illustrated in Figure 5. In this state, the central wall just lifts off from point C and becomes fully supported on the rocking toe at point D, while the force demands in the lumped shear fuses at the left and right spline joints, V_{LT} and V_{RT} , can still be expressed as $V_{LT} = K_0 \Delta_L$ and $V_{RT} = K_0 \Delta_R$ where Δ_L and Δ_R are the shear deformations in these fuses, equal to the relative vertical displacements between adjacent wall panels, as illustrated in Figure 6.

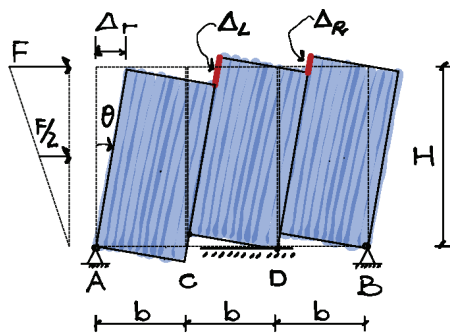


Figure 6. Kinematics of the system

Assuming small rotations and displacements, the shear deformations Δ_L and Δ_R can be evaluated as follows,

$$\Delta_L = 2b \tan \theta \approx 2\Delta_r / \alpha \quad (1)$$

$$\Delta_R = b \tan \theta \approx \Delta_r / \alpha \quad (2)$$

where θ is the rigid-body rotation of the three wall panels resulting from the roof drift Δ_r , and α is the height-to-width aspect ratio of a single panel, defined as H/b . It can be observed that the deformation demand on the left shear fuse is twice that on the right one, resulting in a force ratio, $V_{LT} = 2V_{RT}$. This indicates that if both shear fuses are assigned the same yield strength – as is typically done in practical design – the left shear fuse will yield first, followed shortly by the right one. The inelastic engagement of the shear fuses allows the central wall to undergo the intended rocking motion.

By applying the principle of virtual work or evaluating moment equilibrium for each panel, the lateral stiffnesses, k_{iT} , of the individual panels can be derived and are expressed in Equations (3), (4), and (5):

$$k_{LT} = \frac{F_{LT}}{\Delta_r} = \frac{K_0}{\alpha^2} \left(1.6 - \frac{4}{15} \frac{W}{F_y} \right) \quad (3)$$

$$k_{CT} = \frac{F_{CT}}{\Delta_r} = \frac{K_0}{\alpha^2} \left(1.6 + \frac{4}{15} \frac{W}{F_y} \right) \quad (4)$$

$$k_{RT} = \frac{F_{RT}}{\Delta_r} = \frac{K_0}{\alpha^2} \left(0.8 + \frac{4}{15} \frac{W}{F_y} \right) \quad (5)$$

These equations show that, regardless of the direction of lateral loading, using stiffer shear fuses increases the lateral stiffness of each panel k_{iT} , and thereby the overall stiffness of the wall system. This effect can be achieved more efficiently by introducing stockier wall panels, given the inverse proportionality of k_{iT} to the square of the panels' aspect ratio α^2 .

In addition, tributary gravity loads influence the lateral stiffnesses of the panels in different ways. Irrespective of loading direction, the central panel benefits from the gravity load, gaining additional positive stiffness until its centroid of gravity shifts horizontally beyond the rocking toe – a condition that will be definitely prevented through appropriate design.

In contrast, the influence of gravity on the side panels depends on the direction of lateral loading. For the direction shown in Figure 4, the gravity load on the left panel tends to exacerbate its rotation, introducing negative lateral stiffness, as indicated by the second parenthesized term in Equation (3). This destabilizing effect is counteracted by the shear fuses, which provide positive lateral stiffness and resistance. If the destabilizing effect from gravity exceeds the stabilizing contribution from the fuses, the left panel may display negative lateral stiffness – likely occurring after, rather than before, yielding of the shear fuses.

On the other hand, the tributary gravity load on the right panel acts against its tendency of rotation, contributing positively to its lateral stiffness, along with the stabilizing effect of the shear fuses, as indicated in Equation (5).

Based on the lateral stiffnesses k_{iT} , the tributary lateral loads F_{iT} can be determined by examining the equilibrium conditions of individual panels and the entire system, and are expressed as follows,

$$F_{LT} = \frac{1}{\alpha} \left(0.8F_y - \frac{2}{15}W \right) \quad (6)$$

$$F_{CT} = \frac{1}{\alpha} \left(0.8F_y + \frac{2}{15}W \right) \quad (7)$$

$$F_{RT} = \frac{1}{\alpha} \left(0.4F_y + \frac{2}{15}W \right) \quad (8)$$

By summing these lateral forces resisted by the individual panels, the total base shear of the entire system, V_{b1} , can be obtained at the onset of the first yield in the left shear fuse, as expressed below,

$$V_{b1} = 1.5(F_{LT} + F_{RT} + F_{CT}) = \frac{1}{\alpha}(3F_y + 0.2W) \quad (9)$$

Assuming an elastic–perfectly plastic force–deformation behaviour for the shear fuses, the total base shear, V_{b2} , immediately after the right shear fuse is yielded is given in Equation (10):

$$V_{b2} = \frac{1}{\alpha}(3.6F_y + 0.2W) \quad (10)$$

3 – NUMERICAL INVESTIGATION

3.1 NONLINEAR MODELING

To validate the analytical solutions, a 2D numerical model of a two-story system is developed using OpenSees [18], as shown in *Figure 7a*. Each CLT panel is represented using 4 MITC4 shell elements per story. The effective modulus of elasticity is calculated based on an assumption that only the longitudinal layers contribute to flexural and axial resistance. Furthermore, it is assumed that all lumbers within a layer act monolithically due to bonding effect provided by the perpendicular layers [19].

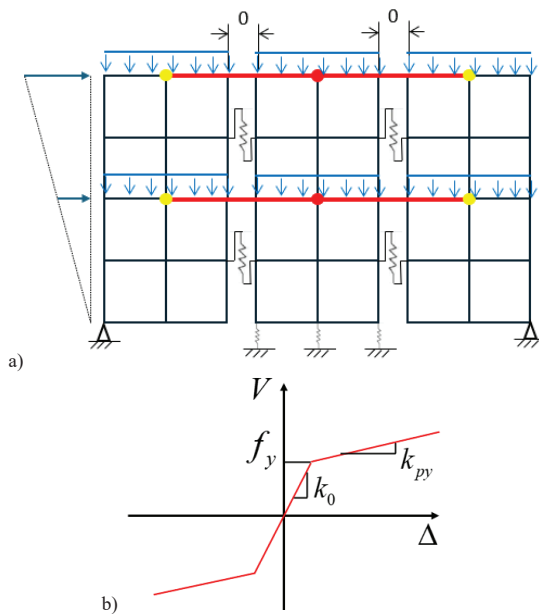


Figure 7. Numerical model of the two-story system a) sketch; b) shear force-deformation relationship of each damper

Within each story, a nonlinear zero-length spring is introduced at mid-height, representing a metallic damper on the spline joint of adjacent two panels. This spring is assigned a bi-linear force-deformation relationship in the vertical direction, characterized by a yield strength f_y , an initial stiffness k_0 , and a post-yield stiffness k_{py} , as illustrated in *Figure 7b*.

The roof and floor slabs are assumed to act as rigid diaphragms, which are implemented using an equalDOF constraint applied in the horizontal direction, with the master node located in the central panel and the slave nodes located in the side panels, as shown in *Figure 7a* using nodes in red and yellow colors respectively.

The free uplifting of the central panel at both rocking toes is modeled through a vertically oriented nonlinear zero-length spring with negligible resistance in tension and very large stiffness in compression. Meanwhile, sliding is restricted at both rocking toes of the central panel. Both side panels are pin-supported at the base through pin connections.

Gravity loads tributary to the three wall panels are applied as a constant uniformly distributed line load at the roof and floor levels. In the horizontal direction, two pointed loads are applied at the roof and floor levels, following a magnitude ratio of 1:0.5, representing a first-mode distribution of seismic inertial forces.

Under these loading conditions, static pushover analysis is conducted in a displacement-controlled manner, with the master nodes at the roof and floor levels adopted as the displacement control points. The maximum roof displacement of 30 mm is reached.

3.2 RESULTS

Figure 8 presents the total base shear versus roof drift where the two inflection points correspond to the onset of yielding in the left dampers (V_{b1}) and the right dampers (V_{b2}), respectively. The values of V_{b1} and V_{b2} obtained from the numerical model closely match those from the analytical model, indicating that the basic assumptions and the derived solutions are valid for the two-story case.

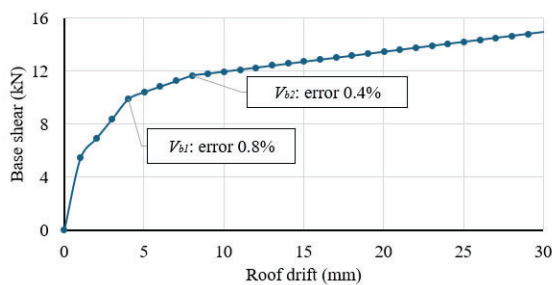


Figure 8. Numerical results of base shear-roof drift relationship

Figure 9 illustrates the shear force-roof drift curves for the upper and lower dampers in the left spline joint. The two curves exhibit nearly identical mechanical response, which suggests that the vertical distribution of damper yield strength can be assigned uniformly in the two-story case.

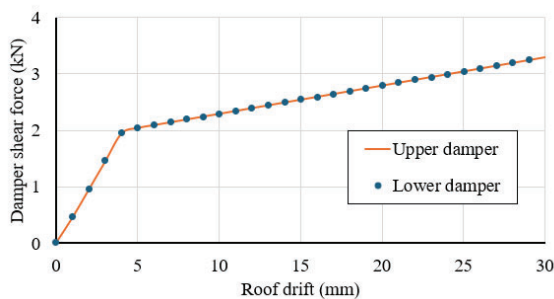


Figure 9. Numerical results of damper shear force history

The displacement profile of the system after the rocking mechanism has been activated is shown in Figure 10. The bending deformation of the CLT panels is negligible compared to the rocking displacements, validating the rigid body assumption adopted in the analytical model for the two-story configuration. Additionally, the size of the circles in the figure represents the shear deformation of each damper. Dampers within the same spline joint exhibit nearly identical shear deformations, further supporting the assignment of uniform yield strength to dampers in the same joint. Furthermore, based on the values indicated by the color bar, the shear deformations of the left and right dampers maintain an approximate 2:1 ratio, consistent with the kinematic relationships derived in Equations (1) and (2).

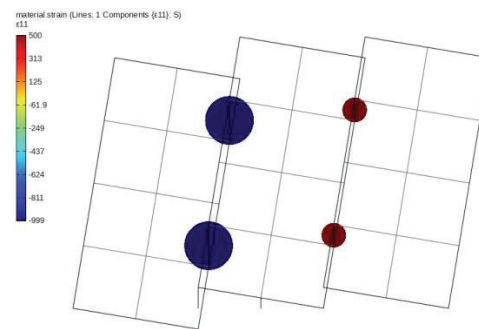


Figure 10. Displacement profiles of the numerical model

4 – CONCLUSION

A novel balloon-framed CLT rocking shear wall system that utilizes non-proprietary yielding fuse plates as energy dissipation devices is introduced and analysed herein. The configuration allows the central panel to rock at its base while the side panels pivot around exterior pin supports, enabling a stable and self-centering seismic response.

Analytical models are developed to describe the base shear capacity and lateral stiffness of the system, accounting for damper and geometric parameters. Validation through nonlinear numerical simulations confirmed that the proposed system delivers accurate stiffness prediction and consistent mechanical response.

The findings provide a promising design solution for seismic applications in mass timber buildings, contributing to the advancement of resilient and sustainable timber engineering practices. Future work will extend the model to dynamic analyses and investigate full-scale experimental validation.

ACKNOWLEDGEMENTS

This research is funded by MITACS Accelerate Grant and sponsorship by Tipping Structural Engineers.

REFERENCES

- [1] American Wood Council (AWC), “National Design Specification for Wood Construction,” Leesburg, VA, USA, 2024.
- [2] American Wood Council (AWC), “Special Design Provisions for Wind and Seismic (SDPWS),” Leesburg, VA, USA, 2021.
- [3] Canadian Standards Association (CSA), “Engineering Design in Wood,” Toronto, Canada, 2024.
- [4] American Society of Civil Engineers (ASCE), “Minimum Design Loads and Associated Criteria for Buildings and Other Structures,” Reston, VA, USA, 2022.

- [5] National Research Council of Canada, "National Building Code of Canada 2020," Ottawa, 2020.
- [6] T. Akbas et al., "Analytical and Experimental Lateral-Load Response of Self-Centering Posttensioned CLT Walls," *Journal of Structural Engineering*, vol. 143, no. 6, Jun. 2017, doi: 10.1061/(ASCE)ST.1943-541X.0001733.
- [7] Z. Chen and M. Popovski, "Structural performance of balloon mass timber shear walls under in-plane lateral loads," *Structures*, vol. 58, p. 105643, Dec. 2023, doi: 10.1016/j.istruc.2023.105643.
- [8] R. Ganey et al., "Experimental Investigation of Self-Centering Cross-Laminated Timber Walls," *J Struct Eng*, vol. 143, no. 10, Oct. 2017, doi: 10.1061/(ASCE)ST.1943-541X.0001877.
- [9] M. A. Kovacs and L. Wiebe, "Controlled Rocking CLT Walls for Buildings in Regions of Moderate Seismicity: Design Procedure and Numerical Collapse Assessment," *J Earthq Eng*, vol. 23, no. 5, pp. 750–770, May 2019, doi: 10.1080/13632469.2017.1326421.
- [10] S. Pei et al., "Simplified Dynamic Model for Post-tensioned Cross - laminated Timber Rocking Walls," *Earthq Eng Struct Dyn*, vol. 50, no. 3, pp. 845–862, Mar. 2021, doi: 10.1002/eqe.3378.
- [11] S. Pei et al., "Experimental Seismic Response of a Resilient 2-Story Mass-Timber Building with Post-Tensioned Rocking Walls," *J Struct Eng*, vol. 145, no. 11, Nov. 2019, doi: 10.1061/(ASCE)ST.1943-541X.0002382.
- [12] A. Hashemi et al., "Seismic resistant rocking coupled walls with innovative Resilient Slip Friction (RSF) joints," *J Constr Steel Res*, vol. 129, pp. 215–226, Feb. 2017, doi: 10.1016/j.jcsr.2016.11.016.
- [13] A. Hashemi et al., "Experimental Testing of Rocking Cross-Laminated Timber Walls with Resilient Slip Friction Joints," *J Struct Eng*, vol. 144, no. 1, Jan. 2018, doi: 10.1061/(ASCE)ST.1943-541X.0001931.
- [14] A. Hashemi et al., "Development of Resilient Seismic Solutions for Timber Structures in New Zealand Using Innovative Connections," *Structural Engineering International*, vol. 30, no. 2, pp. 242–249, Apr. 2020, doi: 10.1080/10168664.2019.1696660.
- [15] C.-P. Lin, R. Wiebe, and J. W. Berman, "Analytical and numerical study of curved-base rocking walls," *Eng Struct*, vol. 197, p. 109397, Oct. 2019, doi: 10.1016/j.engstruct.2019.109397.
- [16] X. Ma et al., "Design and Behavior of Steel Shear Plates with Openings as Energy-Dissipating Fuses," Stanford CA, Mar. 2010.
- [17] M. Ravanbakhshian Habibabadi et al., "Effects of geometric characteristics of U-shaped flexural plates on their cyclic performance," *Structures*, vol. 51, pp. 351–371, May 2023, doi: 10.1016/j.istruc.2023.03.016.
- [18] F. McKenna, "OpenSees: A Framework for Earthquake Engineering Simulation," *Comput Sci Eng*, vol. 13, no. 4, pp. 58–66, 2011.
- [19] Z. Chen and M. Popovski, "Mechanics-based analytical models for balloon-type cross-laminated timber (CLT) shear walls under lateral loads," *Eng Struct*, vol. 208, p. 109916, Apr. 2020, doi: 10.1016/j.engstruct.2019.109916.